

Objective

To explain the phenomenon of synthetic jetting and to demonstrate its application in the pulmonary delivery of dry powder drug candidates.

Introduction

The application of synthetic jetting for pulmonary delivery of drug candidates, for local or systemic targeting, was explored to address a number of desirable pulmonary delivery goals. These include: a) low dose/short drug formulation delivery and b) "near" zero dose independence (less than 10% change in Fine Particle Fraction (FPF) from 15 to 60 L/min). A synthetic jet actuator is a zero-net-mass-flow device, adding momentum (but no mass) to its surroundings (1). Techniques such as finite element analysis (FEA) to predict synthetic jetting from a blower coupled to a piezoelectric transducer (PET), by the formation of a standing acoustic wave, and its impact on aerosol performance, are used to optimize delivery of pulmonary drug candidates. Using these predictions, measurement of the synthetic jet formed was used to infer the resonance frequency of the PET and assist in the optimization of an aerosol delivery system.

Theory

Synthetic Jetting
 Figure 1 shows a schematic of a typical synthetic jet or zero-net mass-flow actuator. In one implementation, a piezoelectric disk is bonded to a metal diaphragm, which is sealed to form a cavity having an orifice or slot. The cavity and/orifice form a Helmholtz resonator. As the diaphragm or driver oscillates, fluid is periodically entrained into and expelled from the orifice. During the expulsion portion of the cycle, a vortex ring can form near the orifice and, under certain operating conditions, covers away from the orifice to form a time-averaged jet. This behavior is often defined as jet formation and was observed more than 50 years ago (1, 2). Figures 1b and 1c show computational fluid dynamic (CFD) analysis verifying the formation of a synthetic jet at a MicroDose blower design.

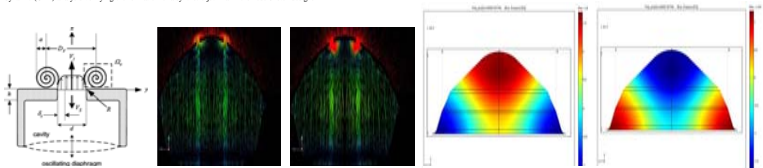


Figure 1: a) Anatomy of a Synthetic Jet, b) CFD Analysis of a Synthetic Jet Expulsion Phase, and c) Inception Phase. Figure 2: Pressure Distribution Inside the Blower During a) Expulsion Phase, b) Inception Phase.

Acoustic Resonance

Acoustic resonance is the tendency of an acoustic system to absorb more energy when the frequency of its oscillations match the system's natural frequency of vibration (its resonance frequency) than it does at other frequencies (3). Blowers must be designed to exhibit acoustic resonance at frequencies close to the PET resonance frequency. The blower shapes are first evaluated using an acoustic Eigenfrequency analysis. This analysis predicts the frequencies at which a given blower shape will acoustically resonate evidenced by the formation of pressure antinodes. This results in an oscillating pressure differential between the air inside the blower holes and the air outside the blower holes. It is this oscillating pressure differential that causes the alternating air jets needed to form a synthetic jet. In Figure 2, the pressure antinodes are shown in blue and red and the pressure nodes are shown in green. Positive pressures are shown in red and negative pressures are shown in blue. Adjacent images show opposite pressure phases.

Synthetic Jetting Measurement

After a blower is designed, validated using acoustic simulation, and manufactured, it is tested using the test fixture shown in Figure 3. The fixture allows for the simultaneous measurement of synthetic jetting strength, PET displacement, and PET Drive Frequency. A sample measurement is shown in Figure 4. The frequency at which maximum synthetic jetting occurs is the acoustic resonance frequency. Blower shapes like those shown in Figure 5 and PET Drive frequencies can be changed to optimize this effect, and consequently, optimize drug delivery and particle size. The correlation between predicted acoustic resonance frequency and measured maximum synthetic jetting frequency is shown in Table 1.

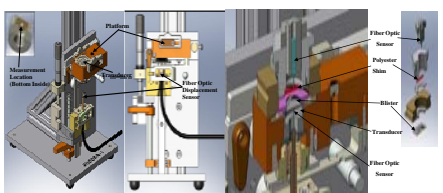


Figure 3: Synthetic Jetting and Transducer Displacement Measurement Fixture

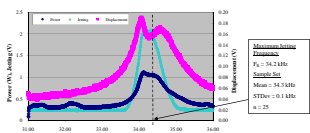


Figure 4: Synthetic Jetting and Transducer Displacement Sample Output

Table 1: Correlation between Predicted Acoustic Resonance Frequency and Measured Maximum Synthetic Jetting Frequency

Blower Type	Maximum Jetting Frequency (kHz)	Predicted Resonance Frequency (kHz)	Difference Between Predicted and Measured (kHz)	% Accuracy
1	54.3	56.4	2.1	93.9%
2	42.8	51.0	8.2	80.6%
3	40.3	48.0	7.7	82.4%
4	38.8	48.1	9.3	80.6%
5	41.2	47.1	5.9	85.7%
6	39.1	45.2	6.1	84.4%
7	38.1	45.4	7.3	86.7%



Figure 5: Various Blower Shapes

Principle of Operation in a MicroDose Inhaler

The device is an active dry powder inhaler which operates with pre-measured single-dose foil blisters, and utilizes a vibration mechanism to deagglomerate the powder within the blisters. The device initiates the actuation process upon detection of a threshold level of inspiratory airflow from the patient, sensed by a directional flow sensor. Upon detection of the inspiration, an electrical drive signal is directed to the PET, which creates vibrations. The vibration of the PET creates ultrasonic standing waves within the blower. These pressure waves cause the powder to be actively deagglomerated, aerosolized, and ejected from the blower through the small orifice. These waves have been passed prior to dosing as shown in Figure 6. The expelled powder is contained into the patient's respiratory branch. Synthetic jets have been most broadly by MicroDose to deliver several classes of drug products, including proteins, peptides, long acting beta agonists, and steroids, formulated as engineered particles, lactose blends and near drug (4).



Figure 6: Stages of Synthetic Jet Formation: Forming, Preceding and Ending

Components and Test Devices

Blisters are sealed using commercial equipment. Filled blisters are sealed and externally packaged as illustrated in Figure 7. The piezoelectric disk is bonded onto the research platform device (Figures 8a and 8b) and performance tested. One option delivery is formulated, research is conducted using the hand-held device with normal jetting (Figure 8c). This device has an independent power source. LED indicators for patient/user feedback, as well as disposable mouthpieces. Illustrations of a potential commercial device are depicted in Figure 9.



Figure 7: Blister Piercing Steps

Figure 8: Various Illustrations of the MicroDose Delivery Platform

Figure 9: Illustrations of a Potential Commercial Device

Materials and Methods

1) Large Molecule
 Spray-dried, neat, peptide formulation (molecular weight approximately 3400) were filled into blisters to provide final dose strengths of 250 µg and 1.5 mg per blister. Blisters were sealed, loaded into the MicroDose-DPE, pierced and actuated using an Anderson Cascade Impactor (ACI) at 150 m/s. The ACI operation comprised of 4 stages through 7 (no plate coating) coupled to a USP selection pan (no pre-operation) and was configured to sample 4L of air. A single blister per strength, was actuated into the ACI, and the stages were extracted using 30%IPA/15%TFA/30%SDS-Water. Samples were injected (100 µL) onto a Phenomenex Jupiter C18 column (50mm x 4.6mm, 5µm packing) and analyzed using UV detection at 200 nm. Sample retention times of 5-6 minutes, at 10 µL/min flow rate, were obtained using a gradient run consisting of the following mobile phases: A: 0.1% TFA/Water, B: 0.1% TFA/Acetronitrile.

2) Small Molecule
 The neat drug substance (1 mg fill weight) and the 25% blend (4 mg fill weight) were manually filled and sealed in blisters, and then individually tested in the device. The Next Generation Impactor (NGI) was used for aerosol performance testing at 30 L/min. Caps were coated with 5% Tween 80 in Methanol. Mobile Phase: 54:46 0.2% TFA in Water; 0.2% TFA in Acetonitrile; Flow: 0.5 mL/min; Injection Volume: 10 µL; Column: Inertsil Phenyl, 5 µm, 100 mm x 3.0 mm, Column Temperature: 50°C; Wavelength of detection: 389 nm, Retention Time: ~2min; Diluent: 3:1 Methanol: Water

Results

1) Large Molecule: Figure 10, Tables 2 and 3, below, display particle size distribution (PSD) and delivered dose uniformity (DDU) data obtained for blisters containing 250 µg and 1500 µg of peptide.

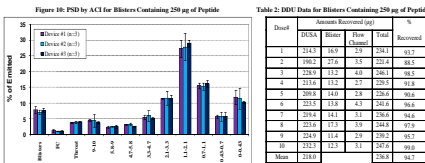


Figure 10: PSD by ACI for Blisters Containing 250 µg of Peptide

Table 2: DDU Data for Blisters Containing 250 µg of Peptide

Dose#	USDA	Blower	Flow	Charted	Returned
1	124.4	200	20	142	10.8
2	190.2	216	35	221.4	84.3
3	228.7	132	48	160.1	69.7
4	219.6	192	24	192	8.4
5	208.9	140	24	220.6	96.9
6	222.7	132	48	160.1	69.7
7	219.6	192	24	192	8.4
8	220.4	171	39	204.9	97.9
9	204.7	132	24	182.2	67.2
10	210.7	192	35	207.9	9.2
Mean	197.8	181	33	210.2	72.9
SD (%)	5.5	1.8	1.8	14.5	7.9

Table 3: DDU Data for Blisters Containing 1500 µg of Peptide

Dose#	USDA	Blower	Flow	Charted	Returned
1	136.2	200	20	142	10.8
2	470.8	192	24	142	10.8
3	113.9	182	24	146	10.7
4	219.6	192	24	192	8.4
5	224.8	190	20	245	10.9
6	222.7	132	48	160.1	69.7
7	219.6	192	24	192	8.4
8	220.4	171	39	204.9	97.9
9	131.1	181	31	147	10.2
10	210.7	192	35	207.9	9.2
Mean	170.8	181	31	145	7.9
SD (%)	11.2	1.8	1.8	14.5	7.9

2) Small Molecule: Figures 11-12 and Table 5, Figures 13-14 and Table 6 display the PSD and DDU data obtained for blisters containing neat drug (1 mg fill weight) and 25% blend (4 mg fill weight), respectively.

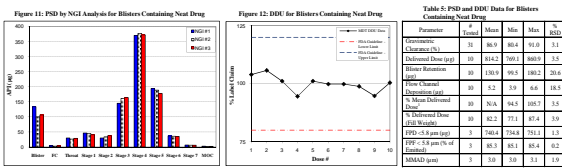


Figure 11: PSD by NGI Analysis for Blisters Containing Neat Drug

Figure 12: DDU for Blisters Containing Neat Drug

Table 5: PSD and DDU Data for Blisters Containing Neat Drug

Parameter	Target	Mean	Min	Max	% (SD)
Flow Rate (L/min)	30	25.8	18.6	30.0	11.3
Charted (%)	100	94.9	86.6	100.0	13.1
Returned (%)	100	138.9	106.5	186.2	26.4
Blower Rotation	100	74.8	64.2	106.5	11.1
Flow Charted (Standard Dev)	100	5.2	1.9	14.4	14.1
% Mean Returned	100	96.8	91.6	100.0	10.8
% Returned Dose (Standard Dev)	100	82.1	71.1	87.4	10.9
FPF (<5 µm) (avg)	7	76.0	74.8	76.0	1.3
FPF (<5 µm) (SD)	1	81.1	81.1	81.1	0.0
MMD (avg)	3	3.0	3.0	3.1	1.0

Figure 13: PSD by NGI Analysis for Blisters Containing 25% Blend

Figure 14: DDU for Blisters Containing 25% Blend

Table 6: PSD and DDU Data for Blisters Containing 25% Blend

Parameter	Target	Mean	Min	Max	% (SD)
Flow Rate (L/min)	30	25.8	18.6	30.0	11.3
Charted (%)	100	94.9	86.6	100.0	13.1
Returned (%)	100	138.9	106.5	186.2	26.4
Blower Rotation	100	74.8	64.2	106.5	11.1
Flow Charted (Standard Dev)	100	5.2	1.9	14.4	14.1
% Mean Returned	100	96.8	91.6	100.0	10.8
% Returned Dose (Standard Dev)	100	82.1	71.1	87.4	10.9
FPF (<5 µm) (avg)	7	76.0	74.8	76.0	1.3
FPF (<5 µm) (SD)	1	81.1	81.1	81.1	0.0
MMD (avg)	3	3.0	3.0	3.1	1.0

Discussion

Synthetic Jetting and Acoustic Resonance
 The results of acoustic Eigenfrequency analysis yields results between 2.1 kHz and 8.2 kHz higher than the measured maximum jetting frequencies. To better correlate acoustic Eigenfrequency analysis results to experimental data, several improvements need to be made. One improvement would be a more accurate measurement of the internal blower geometry, while another would be a method for measuring the resonance frequency of a blower using an excitation source with a relatively low frequency response over the range of interest.

Large Molecule

- Results show that high and low dose of a peptide can be efficiently delivered using the MicroDose DPE.
- Mean delivered dose values were 87% (low dose) to 90% (high dose) of labeled amount.
- FPF values of approximately 85% (meant <4.7 microns) were obtained.
- Aerosol performance was essentially flow rate independent as demonstrated by the small change in FPD (measured using ACI) exhibited for the low strength dose at 15 to 60 L/min flow rates.

Small Molecule

- A representative small molecule was delivered efficiently both as a neat sample of the drug substance alone, as well as from a proportionally equivalent blend also containing excipients such as lactose.
- Mean delivered dose values were 81% for the neat drug substance and 82% for the blended formulation of labeled amount.
- FPF values of approximately 85% (meant <5.8 microns) were obtained for both neat and formulated material.

Conclusion

The novel application of synthetic jetting for the delivery of a peptide and a small molecule was demonstrated to provide highly efficient delivery and desirable attributes of formulation flexibility including delivery of low dose/short drug and near flow rate independence.

References

1) Holman R., and Urtukar U., (2005). "Formation Criterion for Synthetic Jets," AIAA Vol. 43 (10).
 2) Inagui U., and Labare S., (2004). "Acoustic Circulation Effects and the Nonlinear Impedance of Orifices," *J. Acoustical Society of America*, Vol. 22, No. 2, 1950, pp. 211-213.
 3) Kinler L., Frey A., Copepen A., and Sanders J., (2000). *Fundamentals of Acoustics 4th Edition*. NYC: John Wiley & Sons, Inc. pp. 48.
 4) Brown B., Ramonson J., Becker D., and Friend D., (2004). "A Piezo-Electric Inhaler for Local & Systemic Applications," *Drug Del. Technol.*, Oct. 2004 (48), pp. 90-93.